Pramana – J. Phys. (2022) 96:209
https://doi.org/10.1007/s12043-022-02456-2

Effect of different nucleon–nucleon interactions based on relativistic mean field theory on elastic scattering cross-sections of proton and neutron halo nuclei

M AYGUN

Department of Physics, Bitlis Eren University, 13000 Bitlis, Turkey
E-mail: murata.25@gmail.com

MS received 8 January 2022; revised 22 March 2022; accepted 4 July 2022

Abstract. In our study, a comparative analysis of different nucleon–nucleon (NN) interactions which are produced within the relativistic mean field (RMF) theory is performed under the optical model. The real potential is obtained using the double-folding model for four different effective NN interactions such as R3Y(HS), R3Y(Z), R3Y(W) and R3Y(L1). The theoretical results are compared with M3Y effective NN interaction results which are calculated using this work. The similarities and differences of the NN interactions are discussed, and alternative NN interactions to M3Y are suggested.

Keywords. Relativistic mean field; nucleon–nucleon interaction; optical model; double-folding model.

PACS Nos 13.75.Cs; 24.10.Ht

1. Introduction

Nucleus–nucleus potential plays a very important role in obtaining information about the structure and dynamics of nuclei. In this way, the optical model is one of the most used models although there are different models to achieve the potential [1–3]. It consists of the real and imaginary potentials. While the imaginary potential is generally selected as Woods–Saxon potential, the real potential can be produced by using a microscopic approach based on the double-folding model which is one of the most popular models. The double-folding model takes into account nucleon–nucleon (NN) interaction as well as density distributions of the projectile and the target nuclei. Therefore, the NN interaction, which has an important place for nuclear force and nuclear structure, is a very significant input in the analysis of a nuclear reaction, and is still a hot topic in nuclear physics [4,5].

Various NN interaction potentials such as Gaussian or Yukawa can be acquired from the literature [6]. Also, different NN interaction potentials have been derived using the relativistic mean field (RMF) theory [7,8]. The RMF theory is one of the microscopic approaches used to find a solution to many-body problem in the field of nuclear physics. It accepts that nucleons interact through meson exchange [9]. The NN interactions have been applied to radioactive decays [7], proton radioactivity [8], fusion reactions [10]. However, we have noticed that the effects of different NN interactions on the elastic scattering cross-sections of proton and neutron halo nuclei have not been examined simultaneously in the literature. Therefore, we believe that it will be important and useful to overcome this deficiency in the literature.

In the present study, we first obtain the real potentials for the R3Y(HS) [11], R3Y(Z) [12], R3Y(W) [12] and R3Y(L1) [12] NN interactions by using the double-folding model. We calculate the elastic scattering cross-sections of the ^{6}He $+^{12}$C, ^{11}Li $+^{12}$C, ^{11}Be $+^{12}$C, ^{8}B $+^{208}$Pb, ^{9}C $+^{208}$Pb and ^{17}F $+^{58}$Ni reactions for the imaginary potential with the Woods–Saxon potential. Then, we perform the theoretical calculations for the M3Y effective NN interaction to make a comparative study. Finally, we focus on the similarities and differences of the NN interactions, and propose alternative NN interactions that explain the elastic scattering experimental data of the proton and neutron halo nuclei.

Published online: 18 October 2022

2. Theoretical formalism

2.1 *Calculation procedure*

The total potential (V_{Total}) can be defined as

$$V_{\text{Total}}(r) = V_{\text{Coulomb}}(r) + V_{\text{Nuclear}}(r). \quad (1)$$

The $V_{\text{Coulomb}}(r)$ potential [13] is accepted as

$$V_C(r) = \frac{1}{4\pi\epsilon_\circ}\frac{Z_P Z_T e^2}{r}, \quad r \geq R_c, \quad (2)$$

$$= \frac{1}{4\pi\epsilon_\circ}\frac{Z_P Z_T e^2}{2R_c}\left(3 - \frac{r^2}{R_c^2}\right), \quad r < R_c, \quad (3)$$

where R_c is the Coulomb radius, $Z_P(Z_T)$ indicates the charge of the projectile(target) nucleus, respectively. The $V_{\text{Nuclear}}(r)$ potential is the sum of the real and imaginary potentials. The real potential is formed with the help of the double-folding potential given by

$$V(\vec{r}) = N_R \int \mathrm{d}\vec{r}_1 \times \int \mathrm{d}\vec{r}_2 \rho_P(\vec{r}_1)\rho_T(\vec{r}_2)\nu_{NN}[\vec{r} - (\vec{r}_1 - \vec{r}_2)], \quad (4)$$

where N_R is the renormalisation factor, $\rho_{P(T)}(\vec{r}_{1(2)})$ is the density of the projectile(target) and ν_{NN} is the nucleon–nucleon interaction. For all the projectiles, we have used the São Paulo (SP) density distribution shown by [14]

$$\rho_i(r) = \frac{\rho_{0i}}{1+\exp\left(\frac{r-R_i}{a_i}\right)}, \quad i = n \text{ (neutron)}, \quad p \text{ (proton)}, \quad (5)$$

where

$$R_n = 1.49N^{1/3} - 0.79, \quad a_n = 0.47 + 0.00046N, \quad (6)$$

$$R_p = 1.81Z^{1/3} - 1.12, \quad a_p = 0.47 - 0.00083Z. \quad (7)$$

The density of ^{12}C target can be calculated using

$$\rho(r) = (\xi + \gamma r^2)\exp(-\beta r^2), \quad (8)$$

where $\xi = 0.1644\,\text{fm}^{-3}$, $\gamma = 0.082003\,\text{fm}^{-2}$ and $\beta = 0.3741\,\text{fm}^{-2}$ [15]. The densities of ^{58}Ni and ^{208}Pb targets are based on the two-parameter Fermi (2pF) density formulated by

$$\rho(r) = \frac{\rho_0}{1+\exp\left(\frac{r-c}{z}\right)}, \quad (9)$$

where $\rho_0 = 0.172\,\text{fm}^{-3}$, $c = 4.094$ fm, $z = 0.54$ fm for ^{58}Ni [16], and $\rho_0 = 0.1600\,\text{fm}^{-3}$, $c = 6.62$ fm, $z = 0.551$ fm for ^{208}Pb [17]. The imaginary potential is accepted in the Woods–Saxon shape given by

$$W(r) = -\frac{W_0}{1+\exp\left(\frac{r-r_w\,(A_P^{1/3}+A_T^{1/3})}{a_w}\right)}, \quad (10)$$

where W_0, r_w and a_w are the depth, radius and diffuseness parameters. The codes DFPOT [18] and FRESCO [19], respectively are used in the double-folding model and the optical model calculations.

2.2 *Microscopic NN interaction*

The effective NN interaction can be formulated as the sum of the scalar and vector parts of the single meson fields given by [20–22]

$$\nu_{NN}(r) = \frac{g_w^2}{4\pi}\frac{\mathrm{e}^{-m_w r}}{r} + \frac{g_\rho^2}{4\pi}\frac{\mathrm{e}^{-m_\rho r}}{r} - \frac{g_\sigma^2}{4\pi}\frac{\mathrm{e}^{-m_\sigma r}}{r}, \quad (11)$$

where g_w, g_ρ and g_σ are the coupling constants, and m_w, m_ρ and m_σ are the masses for w, ρ and σ mesons, respectively. If the single nucleon exchange effect is added, eq. (11) becomes

$$\nu_{NN}(r) = \frac{g_w^2}{4\pi}\frac{\mathrm{e}^{-m_w r}}{r} + \frac{g_\rho^2}{4\pi}\frac{\mathrm{e}^{-m_\rho r}}{r} - \frac{g_\sigma^2}{4\pi}\frac{\mathrm{e}^{-m_\sigma r}}{r} + J_{00}(E)\delta(r). \quad (12)$$

The exchange term is written as

$$J_{00}(E) = -276\left[1 - 0.005\frac{E_{\text{Lab}}}{A_p}\right]\text{MeV fm}^3, \quad (13)$$

where E_{Lab} and A_p are the incident energy and mass number of the projectile, respectively. Equation (12) based on the parameters of the R3Y(HS) listed in table 1 becomes [11]

$$\nu_{NN}^{\text{R3Y(HS)}}(r) = 11957\frac{\mathrm{e}^{-3.97r}}{4r} + 4099\frac{\mathrm{e}^{-3.90r}}{4r} - 6883\frac{\mathrm{e}^{-2.64r}}{4r} + J_{00}(E)\delta(r). \quad (14)$$

Then, eq. (12) for the R3Y(Z) parameters transforms [12] as follows:

$$\nu_{NN}^{\text{R3Y(Z)}}(r) = 12009\frac{\mathrm{e}^{-3.96r}}{4r} + 7446\frac{\mathrm{e}^{-3.87r}}{4r} - 7862\frac{\mathrm{e}^{-2.80r}}{4r} + J_{00}(E)\delta(r). \quad (15)$$

Equation (12) for the R3Y(W) parameters becomes [12]

$$\nu_{NN}^{\text{R3Y(W)}}(r) = 8551\frac{\mathrm{e}^{-3.97r}}{4r} - 5750\frac{\mathrm{e}^{-2.79r}}{4r} + J_{00}(E)\delta(r). \quad (16)$$

Table 1. The values of the parameters m_σ (in MeV), m_w (in MeV), m_ρ (in MeV), g_σ, g_w, g_ρ, g_σ^2/π (in MeV), g_w^2/π (in MeV) and g_ρ^2/π (in MeV) of different RMF models including HS, Z, W and L1 interactions.

Parameter	R3Y(HS) [11]	R3(Z) [12]	R3Y(W) [12]	R3Y(L1) [12]
m_σ	520	551.31	550	550
m_w	783	780	783	783
m_ρ	770	763	–	–
g_σ	10.47	11.19	9.57	10.30
g_w	13.80	13.83	11.67	12.60
g_ρ	8.08	10.89	–	–
g_σ^2/π	6882.64	7861.80	5750.24	6660.95
g_w^2/π	11956.94	12008.98	8550.74	9967.88
g_ρ^2/π	4099.06	7445.91	–	–

Table 2. The normalisation constant (N_R), the depth (W_0) in MeV, the radius and diffuseness parameters (r_w and a_w) in fm, the cross-sections (σ) in mb and χ^2/N values for the theoretical analysis with the M3Y, R3Y(HS), R3Y(Z), R3Y(W) and R3Y(L1) effective NN interactions for the neutron and proton halo elastic scattering reactions.

Reaction	V_{NN}	N_R	W_0	r_w	a_w	σ_R	χ^2/N
^{6}He $+^{12}$C	M3Y	1.00	17.0	1.10	0.68	1299	35.6
	R3Y(HS)	1.00	10.0	1.20	0.67	1292	40.6
	R3Y(Z)	1.00	15.0	1.18	0.93	1579	71.6
	R3(W)	1.00	13.0	1.20	0.85	1582	61.3
	R3Y(L1)	1.00	18.0	1.05	0.57	1308	168.0
^{11}Li $+^{12}$C	M3Y	1.00	58.0	1.14	0.40	1183	33.6
	R3Y(HS)	1.00	58.3	1.00	0.40	946	14.9
	R3Y(Z)	1.00	51.0	1.22	0.40	1270	25.2
	R3Y(W)	1.00	51.0	1.25	0.40	1364	43.6
	R3Y(L1)	1.00	55.0	1.26	0.44	1448	40.5
^{11}Be $+^{12}$C	M3Y	1.00	14.0	1.25	0.75	1433	47.6
	R3Y(HS)	1.00	10.0	1.16	0.75	1108	56.1
	R3Y(Z)	1.00	18.0	1.25	0.63	1343	40.5
	R3Y(W)	1.00	23.0	1.29	0.77	1749	73.9
	R3Y(L1)	1.00	28.0	1.25	0.78	1761	87.2
^{8}B $+^{208}$Pb	M3Y	1.00	28.0	1.25	0.96	3785	0.31
	R3Y(HS)	1.00	34.0	1.25	0.90	3748	0.40
	R3Y(Z)	1.00	30.0	1.30	0.82	3700	1.89
	R3Y(W)	1.00	30.0	1.25	0.88	3638	0.20
	R3Y(L1)	1.00	28.0	1.25	0.88	3604	0.17
^{9}C $+^{208}$Pb	M3Y	1.00	95.0	1.26	0.40	3084	0.54
	R3Y(HS)	1.00	30.0	1.32	0.40	3079	0.61
	R3Y(Z)	1.00	55.0	1.26	0.60	3393	0.66
	R3Y(W)	1.00	35.0	1.35	0.30	3095	0.83
	R3Y(L1)	1.00	50.0	1.33	0.30	3077	1.13
^{17}F $+^{58}$Ni	M3Y	1.00	35.0	1.24	0.74	2644	0.38
	R3Y(HS)	1.00	32.5	1.22	0.755	2573	0.54
	R3Y(Z)	1.00	39.0	1.24	0.90	3092	2.47
	R3Y(W)	1.00	23.0	1.33	0.65	2614	0.44
	R3Y(L1)	1.00	25.0	1.33	0.61	2569	0.52

Finally, eq. (12) for the R3Y(L1) parameters is in the following form [12]:

$$v_{NN}^{\mathrm{R3Y(L1)}}(r) = 9968\,\frac{\mathrm{e}^{-3.97r}}{4r} - 6661\,\frac{\mathrm{e}^{-2.79r}}{4r} + J_{00}(E)\delta(r). \quad (17)$$

For the R3Y(W) and R3Y(L1) interactions, only g_w^2/π and g_σ^2/π values are listed in table 1, since the ρ meson contribution is neglected [7]. In order to make a comparative study, we carry out the theoretical calculations for the M3Y effective NN interaction. Thus, we

can discuss the similarities and differences of various NN interactions investigated in this study. The M3Y interaction, which is used in the analysis of numerous nuclear reactions, is one of the most popular interaction potentials. The M3Y effective, which is produced with G-matrix elements under Reid–Elliott soft core NN interaction [23], consists of the sum of three Yukawa potentials with ranges 0.25 fm for a medium-range attractive part and 0.4 fm for a short-range repulsive part. Thus, the M3Y interaction can be written as [24]

$$\nu_{NN}^{\mathrm{M3Y}}(r) = 7999\,\frac{\mathrm{e}^{-4r}}{4r}s - 2134\frac{\mathrm{e}^{-2.5r}}{2.5r} + J_{00}(E)\delta(r). \tag{18}$$

3. Results and discussion

In our study, we have investigated the effects of various NN interaction potentials on the elastic scattering cross-sections of the neutron and proton halo nuclei. The real part of the optical potential has been calculated with the help of the NN interactions and the code DFPOT. The imaginary part of the optical potential has been evaluated as Woods–Saxon potential. In the present study, the double folded potentials together with Woods–Saxon potential as well as the Coulomb potential are used as an input to the FRESCO code which is a Coupled-Channels program evaluated in the cross-section calculations in nuclear physics. Thus, we can calculate the elastic scattering cross-sections by adjusting the imaginary potential parameters. The values of the imaginary potential have been researched at 1.0, 0.1 and 0.01 step intervals to achieve good agreement with the experimental data. We have listed the normalisation constant (N_R), the depth (W_0) in MeV, the radius and diffuseness parameters (r_w and a_w) in fm, the cross-sections (σ) in mb and χ^2/N values for the theoretical analysis with the M3Y, R3Y(HS), R3Y(Z), R3Y(W) and R3Y(L1) effective NN interactions in table 2. Finally, the theoretical calculations have been performed for the determining values.

We have shown the changes as a function of the distance of four different effective R3Y NN interactions as without the $J_{00}(E)$ term in figure 1. For this, the NN interactions have been calculated using the FORTRAN program according to the values given in table 1 for eqs (14)–(17). In addition, we have plotted the M3Y NN interaction for comparison in figure 1. Although the potentials are quite different from each other, especially in the central region, this difference decreases with increasing radial distance. The R3Y(L1) has a deeper structure than other potentials, which makes it more attractive. On the other hand, the R3Y(Z) potential is shallower and less attractive than other potentials. The depths of the R3Y(HS) and R3Y(Z) interactions are very similar to the M3Y interaction. However, the R3Y(W) and R3Y(L1) interactions have a deeper structure than the M3Y interaction. We can say that the differences in the behaviours of the V_{NN} interactions are due to the attractive and repulsive parts depending on the values of the V_{NN} interaction potentials.

3.1 *Real potential depths*

We have shown the changes with the distance of the real parts of nuclear potentials in figure 2. First of all, it can be said that the change in the potentials is the same for both neutron and proton halo nuclei. In this context, the shallowest real potential has been found for the M3Y interaction while the deepest potential is obtained for the R3Y(L1) interaction. It has been observed that both depth and behaviour of R3Y(W) and R3Y(L1) interactions are very close to each other. This situation is an expected result from eqs (16) and (17) where we can obtain the interaction potentials. The R3Y(HS) and R3Y(Z) interactions are far from this situation. While the M3Y, R3Y(W) and R3Y(L1) interactions produce an attractive real potential for the neutron halo nuclei, the R3Y(HS) and R3Y(Z) interactions form a repulsive real potential. This situation is valid for the proton halo nuclei except for the R3Y(HS). Also, the interaction potentials led to a noticeable increase in the real potential depths of the proton halo nuclei. The potential for the R3Y(HS) interaction, which is repulsive for the neutron nuclei, turns into an attractive potential state in the proton halo nuclei. We think that these are due to structural differences such as neutron(s) or proton(s) of the valence nucleon(s) of the halo nuclei.

3.2 *Analysis with neutron halo nuclei*

We have calculated the elastic scattering cross-sections of the ^{6}He $+^{12}$C (at 18 MeV), ^{11}Li $+^{12}$C (at 660 MeV) and ^{11}Be $+^{12}$C (at 422.4 MeV) reactions as the neutron halo nuclei. In order to make a clearer comparison, an energy value for each reaction has been chosen. The theoretical results of ^{6}He $+^{12}$C in figure 3, ^{11}Li $+^{12}$C in figure 4 and ^{11}Be $+^{12}$C in figure 5 have been compared with the experimental data. For the ^{6}He $+$ ^{12}C reaction, the theoretical results are the same for all the NN interactions as well as the M3Y interaction at angles $0^\circ \leq \Theta \leq 19^\circ$ while the differences among the results arise at forward angles. At the same time,

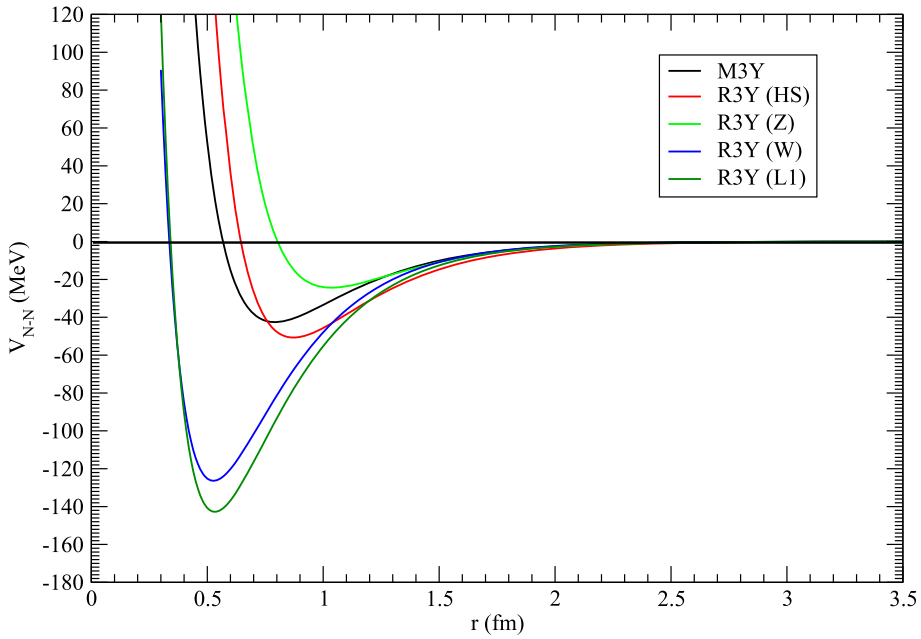

Figure 1. A comparison of the M3Y, R3Y(HS), R3Y(Z), R3Y(W) and R3Y(L1) effective NN interactions as a function of distance.

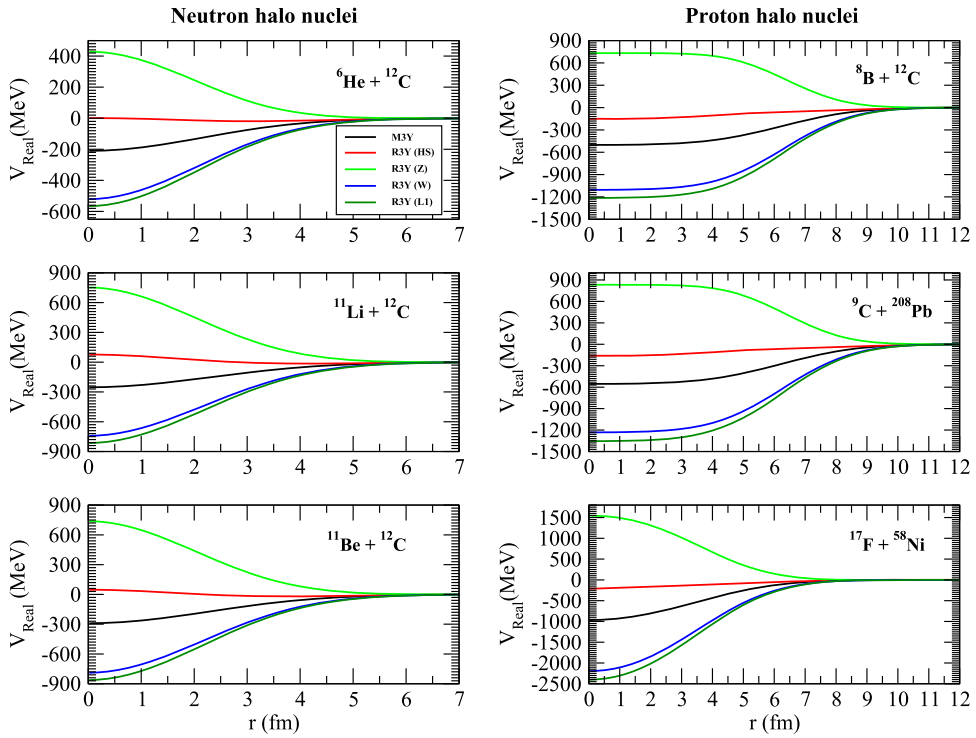

Figure 2. The change with distance of the real potentials calculated using the M3Y, R3Y(HS), R3Y(Z), R3Y(W) and R3Y(L1) effective NN interactions for the neutron and proton halo elastic scattering reactions.

the results with the M3Y and R3Y(HS) interactions are very close to each other. Although the results of the NN interactions in the ^{11}Li + ^{12}C reaction are generally similar, it has been noticed that there is a phase difference among the results. In the ^{11}Be + ^{12}C reaction, the results with the R3Y(W) and R3Y(L1) interactions are very close to each other at all angles. Also, there are no significant differences in the results of the other

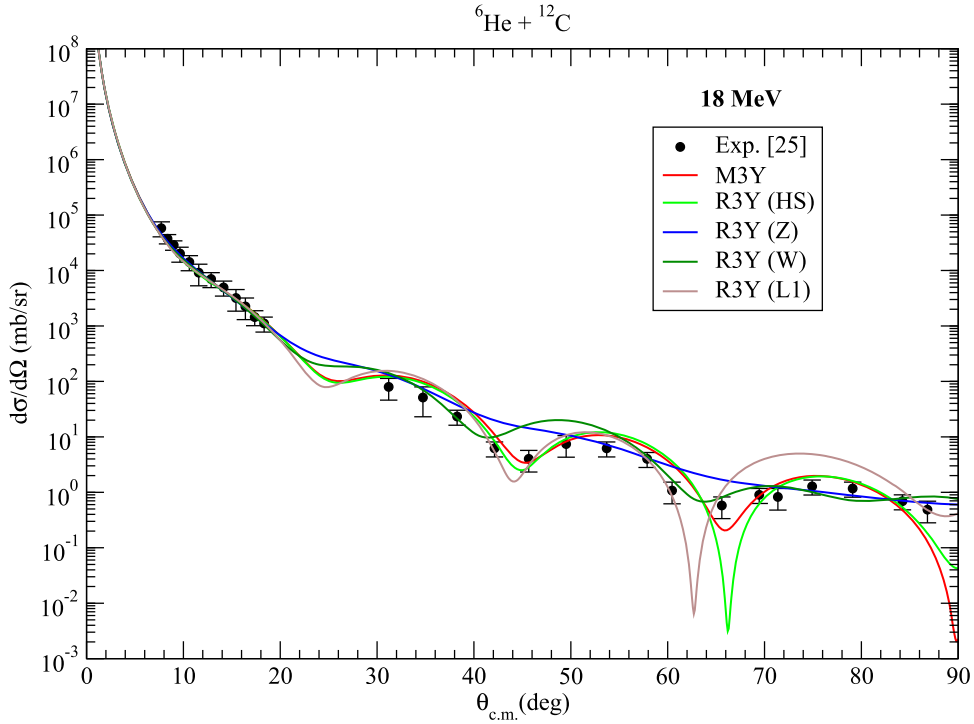

Figure 3. The elastic scattering cross-sections calculated using the M3Y, R3Y(HS), R3Y(Z), R3Y(W) and R3Y(L1) effective NN interactions for ^{6}He $+^{12}$C at 18 MeV [25].

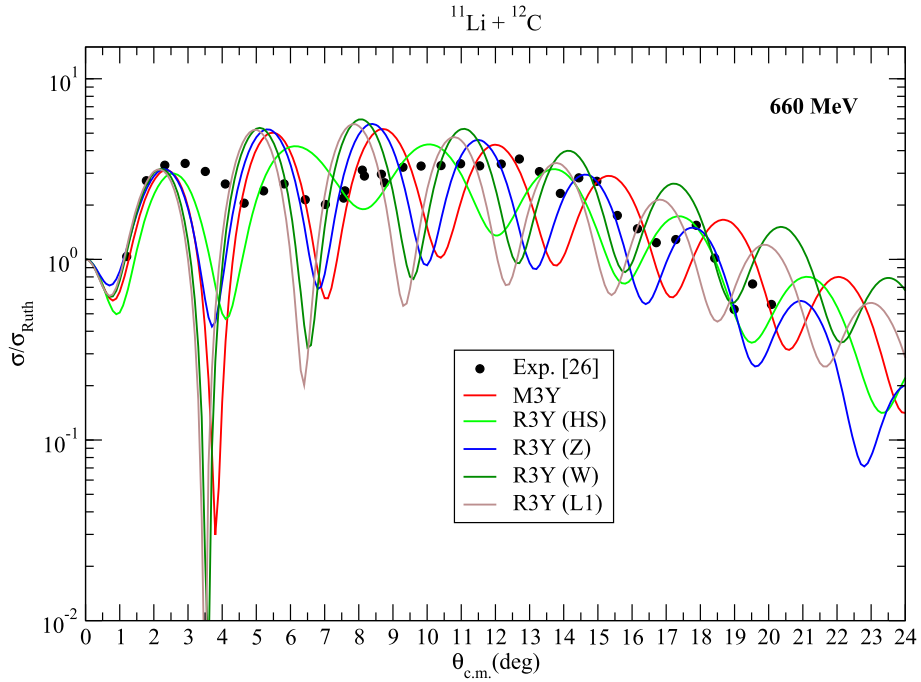

Figure 4. Same as figure 3, but for ^{11}Li + ^{12}C at 660 MeV [26].

NN interactions. A common property of the results with different NN interactions of the neutron halo nuclei is that the R3Y(HS) and R3Y(Z) interactions are compatible with the experimental data, similar to the M3Y interaction. Based on these results, we can say that the R3Y(HS) and R3Y(Z) interactions can be an alternative to the M3Y interaction in explaining the elastic scattering experimental data of the neutron halo nuclei.

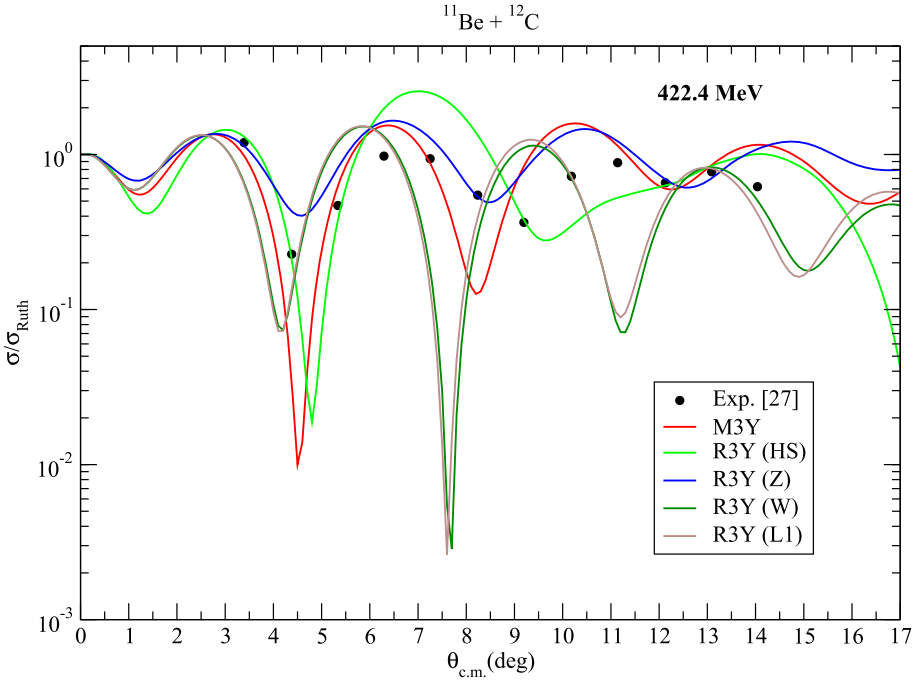

Figure 5. Same as figure 3, but for ^{11}Be + ^{12}C at 422.4 MeV [27].

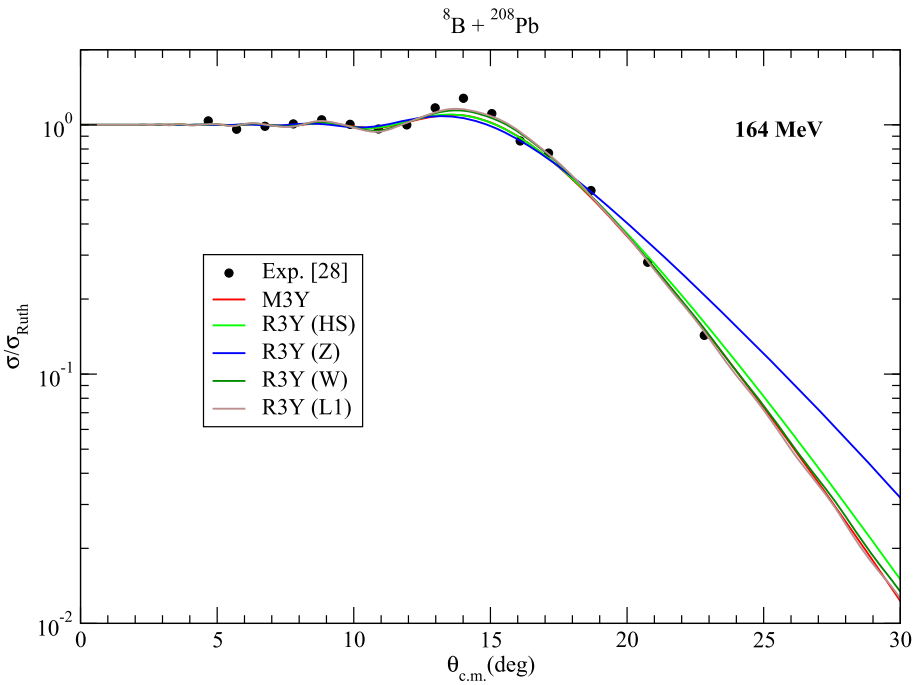

Figure 6. Same as figure 3, but for ^{8}B + ^{208}Pb at 164 MeV [28].

3.3 *Analysis with proton halo nuclei*

We have obtained the elastic cross-sections of the ^{8}B + ^{208}Pb (at 164 MeV), ^{9}C + ^{208}Pb (at 227 MeV) and ^{17}F + ^{58}Ni (at 170 MeV) reactions as proton halo nuclei. We have presented the theoretical results of ^{8}B + ^{208}Pb in figure 6, ^{9}C + ^{208}Pb in figure 7 and ^{17}F + ^{58}Ni in figure 8. In the ^{8}B + ^{208}Pb reaction, the results for the other NN interactions except for the R3Y(Z) interaction are generally very close to each other except for $13^\circ \leq \Theta \leq 17^\circ$. For the ^{9}C + ^{208}Pb reaction, the results with the R3Y(HS) and M3Y interactions are close to each other while the results of the R3Y(W) and R3Y(L1) interactions show a close behaviour. On

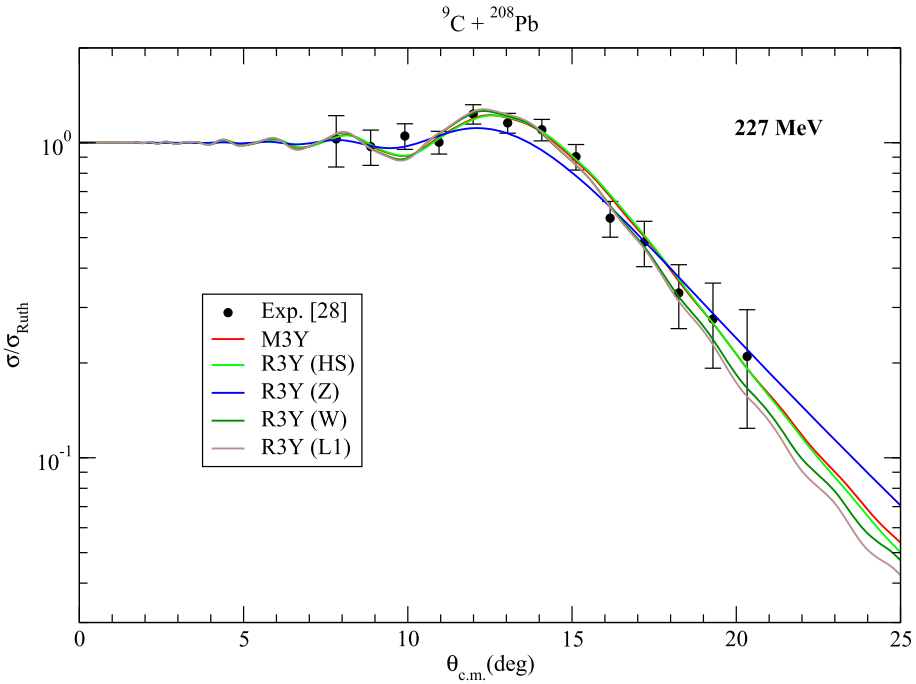

Figure 7. Same as figure 3, but for ^{9}C + ^{208}Pb at 227 MeV [28].

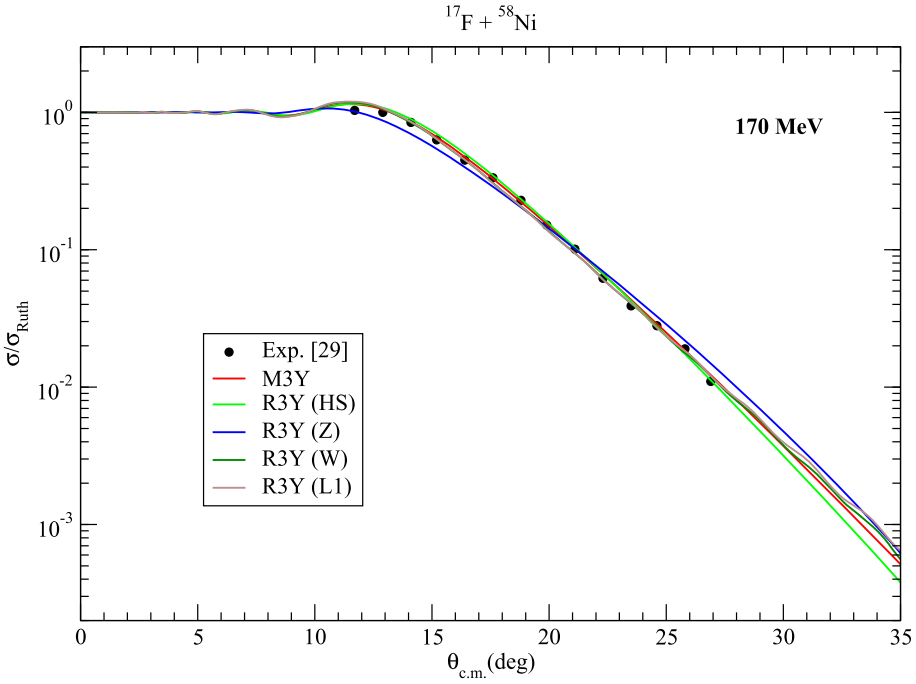

Figure 8. Same as figure 3, but for ^{17}F + ^{58}Ni at 170 MeV [29].

the other hand, the R3Y(Z) interaction exhibits a different behaviour compared to the other NN interactions. In the ^{17}F +^{58}Ni system, the results of the other NN interactions except for the R3Y(Z) interaction are very similar to each other in general. Consequently, we have noticed that the NN interaction potentials except for the R3Y(Z) interactions have given similar results to each other, and are also in very good agreement with the experimental data. Therefore, we can deduce that the R3Y(HS), R3Y(W) and R3Y(L1) NN interactions

can be a good alternative to the M3Y NN interaction in the analysis of the elastic scattering cross-sections of the proton halo nuclei.

4. Summary and conclusions

In the present study, we have investigated the probable correlations among four different NN interaction potentials which comprise of R3Y (HS), R3Y (Z), R3Y (W) and R3Y (L1). We have calculated the elastic scattering cross-sections of the neutron and proton halo reactions such as ^{6}He $+^{12}$C, ^{11}Li $+^{12}$C, ^{11}Be $+^{12}$C, ^{8}B $+^{208}$Pb, ^{9}C $+^{208}$Pb and ^{17}F $+^{58}$Ni. We have observed that the R3Y(HS), R3Y(W) and R3Y(L1) interactions for the analysis of the proton halo nuclei, and the R3Y(HS) and R3Y(Z) interactions for the analysis of the neutron halo nuclei can be a good alternative to the M3Y interaction. One of the reasons for this is that the depths of the R3Y(HS) and R3Y(Z) NN interactions are very similar to the M3Y interaction, as can be seen from figure 1. Consequently, we can deduce from the analysis of both proton and neutron reactions that the R3Y(HS) interaction can be an alternative interaction to the M3Y interaction. We believe that it would be interesting and useful to apply these interactions to nuclear reactions such as inelastic scattering and transfer.

References

[1] M Aygun, *Pramana – J. Phys.* **94**, 104 (2020)
[2] M Aygun, *Pramana – J. Phys.* **93**, 72 (2019)
[3] M Aygun, *Pramana – J. Phys.* **88**, 53 (2017)
[4] B B Sahu, S K Singh, M Bhuyan and S K Patra, *Pramana – J. Phys.* **82**, 4 (2014)
[5] C Lahiri, S K Biswal and S K Patra, *Int. J. Mod. Phys. E* **25**, 1650015 (2016)
[6] M Bhuyan and R Kumar, *Phys. Rev. C* **98**, 054610 (2018)
[7] B Singh, M Bhuyan, S K Patra and R K Gupta, *J. Phys. G: Nucl. Part. Phys.* **39**, 025101 (2012)
[8] B B Sahu, S K Singh, M Bhuyan, S K Biswal and S K Patra, *Phys. Rev. C* **89**, 034614 (2014)
[9] M Kaur, A Quddus, A Kumar, M Bhuyan and S K Patra, *J. Phys. G: Nucl. Part. Phys.* **47**, 105102 (2020)
[10] M Bhuyan, R Kumar, S Rana, D Jain, S K Patra and B V Carlson, *Phys. Rev. C* **101**, 044603 (2020)
[11] C J Horowitz and B D Serot, *Nucl. Phys. A* **368**, 503 (1981)
[12] P G Reinhard, *Rep. Prog. Phys.* **52**, 439 (1989)
[13] G R Satchler, *Direct nuclear reactions* (Oxford University Press, Oxford, 1983)
[14] L C Chamon, B V Carlson, L R Gasques, D Pereira, C De Conti, M A G Alvarez, M S Hussein, M A C Ribeiro, E S Rossi, Jr and C P Silva, *Phys. Rev. C* **66**, 014610 (2002)
[15] S Qing-biao, F Da-chum and Z Yi-zhong, *Phys. Rev. C* **43**, 2773 (1991)
[16] M El-Azab Farid and M A Hassanain, *Nucl. Phys. A* **678**, 39 (2000)
[17] S Hossain, M N A Abdullah, Md Z Rahman, A K Basak and F B Malik, *Phys. Scr.* **87**, 015201 (2013)
[18] J Cook, *Commun. Comput. Phys.* **25**, 125 (1982)
[19] I J Thompson, *Comput. Phys. Rep.* **7**, 167 (1988)
[20] R Brockmann, *Phys. Rev. C* **18**, 1510 (1978)
[21] L D Miller and A E S Green, *Phys. Rev. C* **5**, 241 (1972)
[22] R Brockmann and W Weise, *Phys. Rev. C* **16**, 1282 (1977)
[23] J Boguta and A R Bodmer, *Nucl. Phys. A* **292**, 413 (1977)
[24] G R Satchler and W G Love, *Phys. Rep.* **55**, 183 (1979)
[25] M Milin *et al*, *Nucl. Phys. A* **730**, 285 (2004)
[26] J J Kolata *et al*, *Phys. Rev. Lett.* **69**, 2631 (1992)
[27] V L Strowski *et al*, *Phys. Lett. B* **658**, 198 (2008)
[28] https://www-nds.iaea.org/exfor/
[29] J F Liang *et al*, *Phys. Lett. B* **681**, 22 (2009)